The effect of rising atmospheric oxygen on carbon and sulfur isotope anomalies in the Neoproterozoic Johnnie Formation, Death Valley, USA

Alan J. Kaufman[1], Frank A. Corsetti[2], and Michael A. Varni[1]

[1]The University of Maryland, Geology Department, College Park, MD 20742-4211

[2]The University of Southern California, Department of Earth Sciences, Los Angeles, CA 90089

Abstract

Carbonates within the Rainstorm Member in the terminal Neoproterozoic Johnnie Formation of Death Valley, California record a remarkable negative carbon isotope anomaly – to a nadir of near -11‰ – that accompanies a dramatic rise in trace sulfate abundance and fall of carbonate associated sulfate $\delta^{34}S$ values. The carbonates, including the laterally extensive Johnnie Oolite, were deposited during marine flooding atop a sequence boundary best observed in cratonward sections. The ^{12}C-rich alkalinity delivered to the seawater pool was likely associated with a dramatic rise in atmospheric O_2, which resulted in 1) the oxidation of exposed continental shelf sediments rich in fossil organic matter and sulfides, and 2) the ventilation of the oceans. The carbon isotope anomaly is recorded in broadly equivalent successions that post-date known Marinoan glacial deposits and pre-date the Precambrian-Cambrian boundary in Oman, India, China, Australia, and Namibia, supporting the view that the oxygenation event was global. Large metazoan fossils (Ediacaran animals) first appear directly above this anomaly, suggesting that a critical threshold with respect to atmospheric O_2 had been crossed at this time. A negative excursion of similar magnitude occurs in overlying strata at the Precambrian-Cambrian boundary, which likely reflects similar processes.

1. Introduction

The rise and fall of atmospheric oxygen through geological time is related to globally averaged processes that produce and sequester oxidants, including primary productivity and sedimentation, as well as tectonic forces that affect weathering, erosion, and hydrothermal

activity (Berner, 2001 and references therein). Stratigraphic fluctuations of carbon and sulfur isotopes in seawater proxies, which monitor the balance between burial and oxidation of organic matter and pyrite, reflect these processes, (e.g., Claypool et al., 1980; Holser, 1984; Hayes et al., 1999). If these isotopic systems are linked, net losses of O_2 from the atmosphere would be associated with periods of oxidative weathering (providing alkalinity and sulfate to seawater), while net gains in atmospheric O_2 occur when reduced carbon and sulfur, as pyrite, are sequestered through biological and physical pathways into sediments (Des Marais et al., 1992; Derry et al., 1992). Insofar as the end of the Proterozoic Eon is considered a time of rapid buildup of atmospheric oxygen, it is not surprising that extreme $\delta^{13}C$, $\delta^{34}S$ and $^{87}Sr/^{86}Sr$ anomalies in seawater proxies typify the Neoproterozoic Earth (Knoll et al., 1986; Derry et al., 1992; Kaufman et al., 1993; Kaufman and Knoll, 1995; Canfield and Teske, 1996). What is notable is that the rise in oxygen may have broadly coincided with deglaciation *and* early animal evolution, potentially within 20 million years of the Precambrian-Cambrian boundary (Kaufman and Hebert, 2003; Bowring et al., 2003).

The general absence of bedded sulfates throughout the Neoproterozoic Era, however, results in a low resolution and temporally uncertain view of seawater sulfur isotope variations (*cf.* Strauss, 1993; 1997); more detailed understanding of the system requires that other proxies be developed to elucidate seawater $\delta^{34}S$ through time. Recently, several groups have converged on a technique to isolate and analyze structurally bound sulfate in both modern (Burdett et al., 1989) and ancient carbonates (Kamshulte et al., 2001; Gellatly et al., 2001; Hurtgen et al., 2002; Kampshulte and Strauss, 2004; Newton et al., 2004). A number of these studies have revealed remarkably rapid and unprecedented changes in both carbon

and sulfur isotopes, in particular associated with post-glacial cap carbonates of the Neoproterozoic (Varni et al., 2001; Hurtgen et al., 2002; Kaufman et al., 2002).

The thick and fossiliferous Neoproterozoic succession in Death Valley, California, provides an opportunity to examine the remarkable carbon and sulfur isotopic records associated with terminal Proterozoic events. Here, significant biogeochemical anomalies are found in cap carbonates atop glacial diamictite in the Kingston Peak Formation and Noonday Dolomite, as well as in other horizons containing cap carbonate-like lithofacies for which glacial strata are not observed (Corsetti and Kaufman, 2003). The youngest and most profound negative $\delta^{13}C$ excursion in the succession (as low as -11‰ vs. VPDB) is recorded in the uppermost Johnnie Formation, which lacks evidence for contemporaneous glaciation and sits stratigraphically below Ediacaran-bearing beds. If primary, this biogeochemical anomaly requires an additional source of ^{12}C-rich alkalinity to the seawater pool.

To better understand the cause of the unprecedented terminal Neoproterozoic $\delta^{13}C$ excursion and its relationship to fluctuations in sea level, atmospheric gases and the evolution of metazoa, new field relationships, mineralogical investigations, and carbonate associated sulfate (CAS) studies were undertaken on the Johnnie Formation in the Death Valley succession.

2. Geologic Observations

The Neoproterozoic Johnnie Formation in Death Valley, California, was deposited in a siliciclastic-dominated, post-rift, predominantly-passive margin setting with minor fluvial influence during the terminal Neoproterozoic (Stewart, 1970; 1982; Benmore, 1974, 1978; Summa et al., 1991; Summa et al., 1993a, b). The top of the formation is subdivided into the

Rainstorm Member, which consists of siltstone, quartzite and minor carbonate, including the two-meter thick Johnnie Oolite (Fig. 1a, b) and a series of thinly bedded pink arenaceous limestone. The post-oolite Rainstorm Member contains a sequence of hummocky cross-stratified and interference ripple cross-laminated quartzite, siltstone, and shale with local preservation of pink carbonates. The beds continue for more than 50 meters in some exposures, and contain oolitic, intraclastic or peloidal grainstones. Notably, the pink carbonates (Fig. 1c) are punctuated by gray limestones characterized by calcite pseudomorphs of small aragonite crystal fans that apparently grew on the ancient seafloor (Fig. 1d; Pruss and Corsetti, 2002; Corsetti et al., in press).

The Rainstorm Member carbonates are incised by a regionally significant sequence boundary with as much as 150 m of local erosional relief (Summa, 1993; Clapham and Corsetti, 2004). Incised valley fill consists of a sandy to muddy matrix with sub-angular blocks of varied lithology, including lower Johnnie stromatolitic carbonate and giant ooids from the Beck Spring Dolomite, found more than a kilometer lower in the section (Summa, 1993; Corsetti and Kaufman, 2003). Above the incision, the post-Rainstorm Johnnie Formation consists of featureless dark green mudstones (Stewart, 1970; Moore, 1974; Charlton et al., 1997) that become progressively sandy up section to the contact with the overlying Stirling Quartzite. A dark finely laminated micritic limestone is also found in this interval in the Nopah Range.

The age of the Johnnie Formation is bracketed between Mesoproterozoic sills found in the far underlying Crystal Spring Formation (1.087 Ga; Heaman and Grotzinger, 1991) and the presence of the terminal Proterozoic index fossil *Cloudina* in the overlying Stirling

Quartzite (Hagadorn et al., 2000; *Cloundina* is known elsewhere to occur between ~548 and the Precambrian-Cambrian boundary at 543 Ma; Grotzinger et al., 1995, which is also preserved in the Death Valley area; Corsetti and Hagadorn, 2000). Tighter constraints are permissible given that underlying glacial deposits and cap carbonate of the Kingston Peak and Noonday Dolomite formations are generally assigned to the Marinoan ice age, which is constrained in Chinese successions to be younger than 663 +/- 4 (Zhou et al., 2004). Alternatively, Christie-Blick and Levy (1989) and Abolins et al. (2000) correlate the post-Rainstorm incision via sequence stratigraphic methods to the Neoproterozoic succession in Utah. If their assignment is correct, the pre-incision carbonate beds are likely to be older than 580 Ma, the age of volcanics of the Brown's Hole Formation, Utah, which lie stratigraphically above the sequence boundary.

In most sections, the remarkably widespread Johnnie Oolite sharply overlies green and purple shale with no apparent discontinuity. The surface between these two disparate lithologies has been interpreted to represent a cryptic unconformity (Summa, 1993a, b). Insofar as documentation of this hiatus is important to possible genetic interpretations of the alkalinity event, new observations of this surface were made in a proximal section preserved in the Old Dad Mountains south of Baker, California. The Johnnie Formation is significantly thinner here where it represents the Craton Margin facies of Fedo and Cooper (2001). In continuous outcrop, the Johnnie Oolite is observed to infill grikes and deep pockets of an irregularly eroded grey, stromatolitic dolostone typically found lower in the section (Fig. 1e, f) in more offshore localities. The karst surface at the base of the Johnnie Oolite is interpreted as a notable sequence boundary resulting from sea level drawdown and exposure,

although the magnitude of stratigraphic cutout is unclear due to the attenuation of the cratonal section. Regardless, the new observations demonstrate that the Johnnie Oolite was clearly deposited on a regional disconformity (*cf*. Summa, 1993).

3. Methods

3.1. Carbonates

Stratigraphic samples of the Johnnie Oolite and Rainstorm carbonates were collected from sections in the Mesquite Mountains at Winter's Pass Hills (MM) and Alexander Hills (AR), the southern Nopah Range (Fig. 2), and in more cratonal settings south of Baker, California in the Old Dad Mountains. Samples of the dolomite ooids (not including the surrounding cement), calcite fans and micrite, considered the least altered phases, were isolated by micro-drilling (*cf*. Kaufman et al., 1991); these were reacted for 10 min. at 90^{o}C with anhydrous H_3PO_4 with a Multiprep inlet system in-line with a dual inlet Isoprime gas source mass spectrometer in the Stable Isotope Facility of the University of Maryland Geochemical Laboratories. Isotopic results are expressed in the standard δ notation as permil (‰) deviations from the V-PDB international standard. Uncertainties determined by multiple measurements of a laboratory standard carbonate (calibrated to NBS-19) during each run of samples were better than 0.05‰ for both C and O isotopes.

3.2. Total organic carbon

Concentrations and carbon isotopic compositions of total organic carbon were determined on decalcified residues of powdered whole rock samples by Dumas combustion at 850^{o}C for 2 h with CuO as an oxidant in evacuated and sealed Vycor tubing. The CO_2

formed from the combustion was distilled from H_2O by cryogenic distillation, quantified, and then packaged for mass spectrometric analysis on the dual inlet Isoprime mass spectrometer. Results are reported as mgC/g sample (calculated from CO_2 yields) for concentration, and as above for carbon isotope composition. Uncertainties based on multiple extraction and analyses of a standard carbonate are better than 0.15 mgC/ g sample and 0.3‰ for concentration and carbon isotope composition, respectively.

3.3. Carbonate associated sulfate (CAS)

Structurally bound sulfate was extracted from 50 to 100 grams of finely ground whole rock powder through a series of leaching and dissolution steps (*cf.* Burdett et al., 1989). Fine powders were initially leached for 24 hours in ultra-pure Milli-Q water to remove any sedimentary sulfate, sulfate in fluid inclusions, or sulfate formed by the oxidation of pyrite. This step was followed by a 24-hour leach in 5.25% NaOCl (bleach) to release sulfur bound to organic constituents and metastable sulfides. Powders were sequentially washed and decanted (2 to 3 times) with Milli-Q water prior to quantitative dissolution of carbonate with distilled 3M HCl. The supernatant was separated from the bulk of the insoluble residues by gravity filtration through a coarse Whatman filter. A second filtration was conducted by aspiration through a 4.5-micron Supor brand filter to remove any residual particulates from the solution. Insoluble residues were dried, quantified, and characterized by XRD and electron microprobe techniques. Trace sulfate in the 3M HCl solutions were heated to near boiling and then ~50 ml of a 30% $BaCl_2$ solution was added to initiate precipitation of insoluble barite. The solutions were allowed to cool to ambient temperature and sit for 2-3

days to promote further crystallization; precipitates were isolated by aspiration of the solutions through 4.5-micron Supor filters, which were dried in a vacuum desiccator for 24 hours. Barites were carefully scraped off of the filters and quantified, which allowed for minimum estimates of trace sulfate concentration in samples given the potential for losses throughout the extraction procedure (*cf*. Olcott et al., 2004).

A Eurovector elemental analyzer (EA) was used for on-line combustion of barite samples and the separation of SO_2 on-line to a Micromass Isoprime mass spectrometer for $^{34}S/^{32}S$ analyses (*cf*. Grassineau et al., 2001). The effluent from the EA is introduced in a flow of He (80-120 ml/min) to the IRMS through a SGE splitter valve that controls the variable open split. Timed pulses of SO_2 reference gas (99.9% purity, ~ 3nA) are introduced at the beginning of the run using an injector connected to the IRMS with a fixed open ratio split. The isotope ratios of reference and sample peaks are determined by monitoring ion beam intensities relative to background values.

Prepared samples (~500 μgrams) are accurately weighed and folded into small tin cups that are sequentially dropped with a pulsed O_2 purge of 12 ml into a catalytic combustion furnace operating at 1030^{o}C. The frosted quartz reaction tube is packed with granular tungstic oxide on alumina ($WO_3 + Al_2O_3$) and high purity reduced copper wire for quantitative oxidation and O_2 resorption. Water is removed from the combustion products with a 10-cm magnesium perchlorate column, and the SO_2 is separated from other gases with a 0.8-m PTFE GC column packed with Porapak 50-80 mesh heated to 90^{o}C. The cycle time for these analyses was 210 seconds with reference gas injection as a 30-s pulse beginning at 20 seconds. Sample SO_2 pulses begin at 110 seconds and return to baseline values between

150 and 180 seconds, depending on sample size and column conditions. Isotope ratios are determined by comparing integrated peak areas of *m/z* 66 and 64 for the reference and sample SO_2 pulses, relative to the baseline of ~1 x 10^{-11}A. Isotopic results are expressed in the δ notation as per mil (‰) deviations from the CDT standard. Uncertainties of these measurements (± 0.3‰) were determined by multiple analysis of a standard barite (NBS 127) interspersed with the samples.

3.4. X-ray diffraction

The mineralogy of insoluble residues from the trace sulfate extraction was quantified by x-ray diffraction at The George Washington University. For these analyses samples were lightly ground with ethanol, transferred to a glass slides, and allowed to air dry. Prepared slides were scanned with a Scintag XDS 2000 powder diffractometer with a Cu anode and liquid nitrogen cooled Ge solid state detector. Scans were run with an accelerating voltage of 40 kV and current of 45 mA across a range of 3 to 125^{o} 2θ with 5-second steps of 0.02 2θ, requiring ~9 hours per sample. Spectra produced were analyzed using Jade® software; peaks were identified and compared to those of albite, anorthite, hydroxyapatite, barite, kaolinite, muscovite, orthoclase, phlogopite, quartz, and zircon.

3.5. Electron microprobe

The University of Maryland JEOL JXA-8900 Superprobe, a high resolution SEM with combined wavelength and energy dispersive X-ray spectrometers, was used to further characterize compositions of insoluble residues from the trace sulfate extractions.

4. Results

Following general field observations of an upward increase in siliciclastic strata, insoluble residues in the Johnnie Oolite and arenaceous Rainstorm micrites in the Winter's Pass Hills section broadly increase in abundance upsection with a range between 3.7 to 40.1% (Table 1). Petrographic and x-ray diffraction analyses of these samples revealed that the insoluble residues were comprised mostly of angular to sub-rounded quartz grains (>95%) with only minor to trace amounts of feldspar, mica, and clay (Table 2). Electron microprobe scans of the insoluble residues also revealed the occasional presence of abraded zircon as well as micro-nuggets of gold and cassiterite.

Stratigraphic trends in elemental and isotopic abundances in Rainstorm Member carbonates are reported in Table 1; isotopic trends are also shown graphically in Figures 2 and 3. Based on the abundances of insoluble residues, most of the analyzed samples are greater than 80% carbonate. Total organic carbon abundances range between 0.09 and 0.53 mgC/g with oolite samples notably more organic rich than the overlying micrites. CAS abundances, calculated on a siliciclastic-free basis, range widely between 5 and 1490 ppm.

In the most heavily sampled section, the carbon isotopic compositions of Rainstorm Member carbonates begin near -4‰ at the base of the oolite and fall rapidly to a nadir of -11‰ at the base of the overlying micrites (Fig. 3). From here only a slight progressive increase in $\delta^{13}C$ values to near -10‰ is recorded upsection to where the Rainstorm beds are cut out by an amalgamation of the Rainstorm Member incision surface with the basal Stirling Quartzite (Corsetti and Kaufman, 2003). Over the same interval oxygen isotopes in the carbonates are narrowly constrained between -6.3 and -10.9‰. In contrast to the marked ^{13}C

depletion in the carbonate, co-existing organic matter is notably enriched in the heavy isotope with $\delta^{13}C$ values ranging from -16 to -21‰. Calculated magnitudes of fractionation between inorganic and organic carbon (reported as $\Delta\delta$ values) are remarkable low, ranging from 8.8 to 16‰. Sulfur isotopic compositions of CAS co-vary with carbonate carbon isotope abundances. $\delta^{34}S$ values begin near +27‰ in the oolite and then fall precipitously to between +15 and +18‰ in overlying micrites.

Carbonates resting both above and below the pre-Johnnie karst in the cratonal section reveal a narrow range of carbon and oxygen isotope compositions (Table 1; Old Dad Mountains). Oolite values are comparable to the isotopic compositions of ooids in more offshore exposures, while the underlying grey stromatolitic dolomite with a $\delta^{13}C$ value of near to -2.8‰ is most closely matched to middle Johnnie Formation beds some 50 to 75 m lower in thicker sections found elsewhere in the Death Valley region (Corsetti and Kaufman, 2003). In contrast, the thin micritic limestone of the Johnnie Formation in the Nopah Range above the Rainstorm precipitate beds have moderately positive $\delta^{13}C$ values between +2.6 and +2.9‰.

5. Discussion

5.1. Methods

The fine grinding and repeated chemical treatments in the experiments are aimed at releasing all non-structurally bound sulfate, including fluid inclusions and sedimentary sulfate. In many cases the treated carbonate powder will also contain variable amounts of finely-ground pyrite, especially if these are rich in organic matter. Oxidation of pyrite to

sulfate during acidification (3M HCl) is conceivably a problem, however, recent laboratory tests show that this is not a significant process (Olcott et al., 2004). Neither the concentration nor the sulfur isotope abundances of CAS in samples are measurably altered by laboratory pyrite oxidation – supporting the use of CAS as a paleoseawater proxy in well preserved samples.

5.2. *Diagenesis*

Alteration due to recrystallization of ancient carbonates in the presence of metamorphic or meteoric fluids is most often denoted by notable depletions of ^{18}O in measured samples (Banner and Hanson, 1990; Jacobsen and Kaufman, 1999; Corsetti and Kaufman, 2003). While the oxygen isotopic composition of terminal Proterozoic ocean water is not known with great certainty, values around -5‰ are commonly interpreted to reflect depositional conditions (Veizer et al., 1999). Oxygen isotope compositions of micro-samples from Rainstorm Member carbonates that preserve an exceptional record of sedimentary textures (i.e. ooids and seafloor cements) generally fall between -6 and -11‰ (similar to those throughout the Death Valley succession; Corsetti and Kaufman, 2003) suggesting only minor resetting of $\delta^{18}O$ values. In contrast, the organic-rich carbonates *above* the thick Rainstorm precipitate interval record moderately positive $\delta^{13}C$ values and significantly more negative $\delta^{18}O$ compositions. These comparisons suggest that hot fluids moved readily through the mudstone lithofacies, but circumvented the thicker carbonates beneath. Furthermore, organic matter in the upper Rainstorm carbonate samples is not anomalously enriched in ^{13}C, as seen in the underlying organic-poor carbonate lithofacies.

Apparently the remobilization of carbonate and oxidation of organic matter in these clearly more altered Rainstorm carbonates had little effect on $\delta^{13}C$ compositions. Lastly, the stratigraphic coherence of $\delta^{13}C$ trends in carbonate and total organic matter, as well as those in $\delta^{34}S$ of CAS – in this open marine and generally organic poor interval – support the view that depositional trends in these isotope abundances have been well preserved in the Rainstorm interval.

Concentrations of CAS in the Rainstorm carbonates vary significantly. Petrographic analysis reveals variable degrees of neomorphism resulting from inversion of aragonite to calcite, resulting in a spectrum of grain sizes from micrite to microspar (Pruss and Corsetti, 2002). Furthermore the ooids in the Johnnie Oolite have been dolomitized and the whole rock consists of up to 30% cement. Therefore, the wide range of CAS abundances in the Rainstorm carbonates most likely resulted from these secondary processes, and we consider the maximum values to best reflect contemporaneous seawater concentrations. While some sulfate was expelled from the crystal lattice by these processes, the isotopic ratios were not significantly affected (see Hurtgen et al., 2002 for a comparison of interbedded limestone and dolomite CAS abundances, which are notably different while the $\delta^{34}S$ values are equivalent). Our results are consistent with recent studies that demonstrate the original $\delta^{34}S$ in aragonite mud controls the resultant $\delta^{34}S$ even after aggressive inversion from aragonite to calcite in the shallow subsurface (Lyons et al., in press).

5.3. Comparative Earth history

If global in scope, the extreme biogeochemical anomaly recorded in the texturally anomalous Rainstorm carbonates should be preserved worldwide in terminal Neoproterozoic successions above Marinoan glacial deposits and beneath the Precambrian-Cambrian boundary. In fact, remarkably similar negative $\delta^{13}C$ anomalies have been recorded in deep water environments containing mixed shale and carbonate of broadly comparable age in Namibia (Kaufman et al., 1991), South Australia (Pell et al., 1993; Calver, 2000), Oman (Burns and Matter, 1993; Amthor et al., 2003), and India (Kaufman et al., 2000)(Fig. 4), as well as far western (Xiao et al., 2004) and South China (Xiao et al., in press; Kaufman, unpublished data)(Fig. 4). In contrast to the Rainstorm event, which is truncated by incision at Winters Pass, the negative carbon isotope excursions in some of these basinal sections continue for hundreds of meters. None of the anomalies are known to occur immediately above glacial deposits, but all lie above surfaces of unconformity or abrupt flooding (*cf*. Jiang et al., 2002).

The inter-bedding of potentially organic rich shale and carbonate in basinal environments permits the possibility that these excursions may be diagenetic artifacts of the oxidation of organic-rich sediments (Irwin et al., 1977; Kaufman et al., 2000). However, while these intervals are rich in shale, the shales are not remarkably rich in organic matter, and there is no textural evidence for additions of carbonate to the fine-grained chemical sediments (*cf*. Calver, 2000). Supporting the findings of this study, significant enrichment of ^{13}C in organic carbon is also recorded in the intervals of the extreme negative biogeochemical anomalies in India (across the Krol B/C transition; Kaufman et al., 2000) and in South Australia (in the Wonoka Formation; Calver, 2000). Accordingly, the magnitude of

carbon isotope fractionation between inorganic and organic carbon phases is significantly attenuated. A metamorphic origin for organic ^{13}C enrichment (Hayes et al., 1983) and the small fractionation can be ruled out, insofar as organic matter in similar sediments immediately above and below these horizons are not enhanced in the heavy isotope.

In truly organic-rich lithologies from slightly older Neoproterozoic strata in Svalbard and East Greenland (Knoll et al., 1986), Namibia (Kaufman et al., 1991; 1997) and Brazil (Iyer et al., 1995) – where the effects of organic diagenesis would be more likely – both carbonate and organic matter are enriched in ^{13}C, but the expected depositional fractionations are preserved. Given the consistency of $\delta^{13}C$ trends in these terminal Neoproterozoic successions, as well as the localization of the anomaly in the last moments of the Precambrian, organic diagenesis as a cause of the Rainstorm anomaly appears unlikely.

Alternatively, the extreme $\delta^{13}C$ excursion has been interpreted in South Australia to result from basinal isolation and salinity stratification of the water column that resulted in an enhanced $\delta^{13}C$ gradient from surface to deep. For example, in the Wonoka Formation in Bunyeroo Gorge, the extreme anomaly (down to values near -11‰) occurs in sediments potentially related to the infilling of paleo-valleys over a kilometer in depth (von der Borch et al., 1989; Christie-Blick et al., 1990; 1995). If correct, Messinian-style evaporitic lowering of sea level in an isolated basin may have led to the oxidation of deep water column organic matter, thereby driving deep basin alkalinity to the negative $\delta^{13}C$ extremes recorded in Wonoka carbonates (Calver, 2000). Outside of Bunyeroo Gorge, the Wonoka incision is known to cut through the base of the formation into underlying units; in the gorge, evidence for this incision is lacking, although Christie-Blick et al. (1990; 1995) place a cryptic

unconformity at the top of either unit 3 or 4. Insofar as the isotopic trend begins before and is uninterrupted by the proposed hiatus, either its duration must have been short, or the Wonoka negative $\delta^{13}C$ excursion is decoupled from the incision – as is the case for the biogeochemical anomaly in open marine Rainstorm carbonates and the incision that truncates it. Correlation of the very similar carbon isotope events in South Australia and Death Valley, and plate reconstructions that juxtapose the two margins in the Neoproterozoic (AUSWUS; Karlstrom et al., 2001), lead us to the conclusion that the incisions on both cratons, which cut out strata that contain the extreme isotope anomaly, are equivalent and related to tectonic uplift, rather than basin isolation. If the predicted correlations are correct, the biogeochemical anomaly must be younger than ca. 580 Ma, the age of the Acraman impact structure (Schmidt and Williams, 1996; Grey et al., 2003) preserved in sediments immediately beneath the Wonoka Formation.

The strong negative $\delta^{13}C$ trends in the well documented successions in Death Valley, South Australia, India, and China – down to a nadir of -11‰ – do follow the zone of maximal flooding during transgression, supporting the view of a steep seawater depth gradient in $\delta^{13}C$ compositions (Calver, 2000). Enhancement of the isotopic gradient appears to be timed to prior regression, exposure of continental margins, and the sudden influx of ^{13}C-depleted alkalinity to seawater.

5.4. Possible sources of ^{13}C depleted alkalinity

To re-create the remarkable negative carbon isotope anomaly recorded in Rainstorm Member carbonates, an additional flux of carbon-12 rich alkalinity to a well-agitated open marine pool is required. It is most likely that this flux ultimately came from a biological

source. Three sources seem most plausible, including 1) methane in the marine environment, 2) dissolved and particulate organic matter in the oceans, and 3) fossil organic matter trapped in marginal marine sediments.

5.4.1. Methane

Given the magnitude of the negative carbon isotope excursion (nearly 15‰ considering the isotopic composition of pre-Johnnie Oolite carbonates; Corsetti and Kaufman, 2003), the anaerobic oxidation of methane (AOM) in anoxic marine basins seems a likely source of ^{12}C-enriched alkalinity (Reeburgh et al., 1991; Boetius et al., 2000; Valentine, 2002; Wakeham et al., 2004). Methane typically has $\delta^{13}C$ compositions between -60 and -90‰ (Dickens et al., 1995; Kvenvolden et al., 1995) and is produced by methanogens through the breakdown of acetate or the assimilation of hydrogen and carbon dioxide. Fluxes of methane out of seeps and mud volcanoes at the bottom of the present-day Black Sea (Ivanov et al., 1996) result in the highest water column concentration of methane in the world. Little of this methane escapes to the atmosphere, however, as most is consumed by methanotrophs in consortium with sulfate reducing bacteria, resulting in the production of highly ^{13}C-depleted alkalinity and hydrogen sulfide.

Considering the biogeochemical anomaly recorded in the Rainstorm carbonates to be global in scope, mass balance calculations based on modern seawater DIC abundance ($3.17*10^{18}$ moles; Olson et al., 1985) were undertaken. To recreate the negative anomaly of 13‰ (from pre-event carbonates to the first micritic beds above the oolite) would require $8.8*10^{17}$ moles of methane-derived alkalinity to be added to the seawater pool. Given the

modern estimated rate of methane oxidation ($2.8*10^{13}$ moles/year; Fung et al., 1991) and assuming quantitative conversion it would take more than 30,000 years to release the required alkalinity resulting in the biogeochemical anomaly. On the other hand, if seawater DIC concentrations were lower than modern (Bartley and Kah, 2004), the time required to move the terminal Neoproterozoic seawater reservoir to an average value of -10‰ would be proportionally shorter.

Studies of AOM in modern seep environments show positive $\delta^{34}S$ extremes (up to +70‰) in residual pore water sulfate (Aharon and Fu, 2003), and the same is predicted from water column bacterial sulfate reduction in a syntrophic association with archeal methanotrophs. These observations contrast sharply with the strong negative $\delta^{34}S$ trend recorded in the terminal Neoproterozoic example from Death Valley, suggesting that other sources of ^{13}C-depleted alkalinity should be considered. In addition, it is unclear why AOM should have been most prominent during Rainstorm-time, and not in older intervals where AOM has been considered important in cold seep environments (i.e. Neoproterozoic cap carbonates containing seep-like structures; Kennedy et al., 2001; Jacobsen, 2001; Jiang et al., 2004; but for an opposing view see Shapiro, 2002). The well-sorted oolite and arenaceous seafloor cements in the Rainstorm Member are clearly unrelated to a seep environment, supporting the view that the event was oceanographic and widespread. In addition, the ^{13}C enrichment in organic residues from the Rainstorm carbonates is not predicted in environments dominated by methanotrophs.

5.4.2. Dissolved organic matter

In a new view of Neoproterozoic carbon cycling, Rothman et al. (2003) predict that the extreme variations in $\delta^{13}C$ during this interval are the result of high concentrations of dissolved organic matter (DOM) in seawater – aided by widespread anoxia. Under these conditions the deep oceans may also have been sulfidic (cf. Canfield et al., 1998) and likely depleted in ^{34}S. Conversion of photosynthetically produced DOM to ^{13}C-depleted alkalinity requires microbial reprocessing through oxidative metabolisms like respiration, methanotrophy or sulfide oxidation (often at the interface between oxic and anoxic environments), or anaerobic reductive processes including sulfate reduction and denitrification. As noted above, sulfate reduction would most likely result in ^{34}S enrichment of seawater, which is inconsistent with measured values in the Rainstorm carbonates. The oxidative metabolisms, which do produce ^{13}C depleted alkalinity, require higher concentrations of free oxygen in the hydrosphere and atmosphere. In this case, direct abiological oxidation of DOM would also release CO_2 to surface environments, and, at the same time, oxidation of ^{34}S-depleted sulfide from deep in the water column would increase seawater sulfate concentration and lower oceanic $\delta^{34}S$ values. Oxidation of the hydrosphere thus provides a possible solution to coupled isotope events and high sulfate concentrations recorded in the Rainstorm carbonates. While this hypothesis is consistent with the isotopic data, it does not provide an explanation for the widespread alkalinity event as demonstrated by the abrupt occurrence of carbonate seafloor fans in the Johnnie Formation. The significance of the seafloor fans may be local, however, as they have not been recognized in the correlated intervals worldwide, so this hypothesis remains consistent with the known global data.

5.4.3. Fossil organic matter

A third potential source of ^{13}C-depleted alkalinity for the Rainstorm carbonates comes from the oxidation of fossil organic matter in exposed sediments. In particular, fixed organic carbon might have been released to the soils as CO_2 by both biological and atmospheric processes. For example, close examination of exposed organic rich (> 10%) Devonian black shale (Petsch et al., 2000) reveals that some modern bacteria feed directly on fossil organic matter. The CO_2 released by this metabolic process might return to the atmosphere, or react with silicates in the soils to produce alkalinity. A strong negative carbon isotopic shift in seawater may then result as riverine input would be depleted with respect to ^{13}C. A marked increase in atmospheric oxygen would have a similar effect on marine sediments containing abundant fossil organic matter exposed during regression (McKirdy et al., 2001).

Enhanced burial of organic matter over multi-million year intervals is interpreted from the extended record of positive $\delta^{13}C$ extremes in carbonates deposited throughout much of the Neoproterozoic (Knoll et al., 1986; Kaufman et al., 1997; Hoffman et al., 1998). However, near the very end of the era, Pan African orogeny (recorded as a Himalayan scale shift in the strontium isotopic composition of the ocean; Derry et al. 1992; Kaufman et al., 1993) resulted in enhanced continental erosion and marine sedimentation, which accelerated the burial of organic matter and plausibly initiated a remarkable buildup of atmospheric oxygen (Kaufman et al., 1993). Model results suggest that pO_2 may have grown to near

modern concentrations after the last of the Neoproterozoic ice ages, and then declined again around the Precambrian-Cambrian boundary.

A modern analog for a terminal Neoproterozoic coupled oxidation and negative biogeochemical event may be found in recent carbon sequestration experiments by Andrews and Schlesinger (2001). These authors artificially increased CO_2 concentrations around isolated stands of trees by two times over ambient conditions (~700 ppm), and found that CO_2 was enriched in soil beneath the trees by up to 27% over control plots. Over two years the increase of soil CO_2 accelerated rates of silicate weathering, causing a 167% increase of soil alkalinity and proportional increase in dissolved cations. Notably the resultant carbonate alkalinity was depleted in ^{13}C by about -8 to -9‰ relative to the control plots, reflecting the isotopic depletion in the input CO_2.

Similar degrees of ^{13}C depletion in soil alkalinity are predicted from the oxidative release of CO_2 from organic matter. The release, however, would have to be timed with the exposure of organic rich sediments to result in the anomalous negative biogeochemical anomaly. To this end, the documentation of a karst and sequence boundary at the base of the Johnnie Oolite in the cratonal section is critical. Given the similarity of the grey stromatolitic dolomite beneath the karst to carbonates with similar isotopic compositions in the middle of the formation in other sections in Death Valley, sea level fall may have been as much as 50-75 meters (*cf*. Corsetti and Kaufman, 2003).

Lacking physical evidence for glaciation at this time it is not known whether the sea level fall was eustatic or tectonic, but given the extreme biogeochemical anomalies recorded in the ensuing carbonates we prefer to interpret the drawdown in terms of oceanographic

events. In contrast, the later incision (which we interpret as tectonic, based on the lithologic makeup of the valley fill; Corsetti and Kaufman, 2003; after Summa, 1993) has been associated by others with Marinoan glacial eustacy (Christie-Blick and Levy, 1989; Abolins et al., 2000) although physical and chemical evidence of the expected diamictite and cap carbonate is absent.

Support for the terminal Neoproterozoic oxidative hypothesis comes from the close examination of the insoluble residues, CAS abundances and $\delta^{34}S$ compositions. The abundance, texture, and composition of insoluble residues (> 95% angular to sub rounded quartz with minor feldspar and mica and traces of heavy mineral commonly found in lag deposits) in the Rainstorm Member imply a significant flux of wind blown and river-derived siliciclastic material to the margin marine environment. The sudden development of carbonate at a time of strong siliciclastic influx to the basin suggests that alkalinity must have increased during post-incision transgression. With few exceptions, trace sulfate concentrations in older Proterozoic marine carbonates are significantly lower than those recorded in the Rainstorm Member (Hurtgen et al., 2002; Pavlov et al., 2003). Based on these measurements it has been assumed that oceanic sulfate abundance remained low because of widespread anoxia in the oceans (c.f. Canfield). The sudden spike of sulfate abundance in the Rainstorm carbonates thus supports the predicted rise in oxygen in terminal Neoproterozoic surface environments.

The sudden exposure of organic-rich sediments to a more oxidizing atmosphere might have the same general effect on shallow marine carbonates as the microbial oxidation of methane, but would require the input of twice as much carbon, given typical $\delta^{13}C$ values of

organic matter between -25 to -35‰ for the Neoproterozoic (Hayes et al., 1999). Sediments rich in organic matter are also likely to be rich in ^{34}S-depleted pyrite (a mineral that when exposed under a high pO2 atmosphere would likely oxidize along with the organic fraction), releasing sulfate to pore water. The present-day weathering of exposed Phanerozoic black shales indicates a 60 to 100% loss of organic matter and proportional amount of pyrite (Petsch et al., 2000). Rivers transporting the resulting sulfate would enhance seawater concentrations (75% of the sulfate delivered to the oceans comes from rivers) and decrease oceanic $\delta^{34}S$ compositions toward an integrated continental input with sulfur-isotopic composition between +6 to +10‰ (Arthur, 2000).

These isotopic events are plausibly linked to sea level drawdown, exposure of organic-rich platform sediments to elevated atmospheric oxygen, and enhanced riverine inputs of alkalinity derived from the coupled oxidation of fossil organic matter and soil silicate weathering reactions. The significant karst beneath the Johnnie Oolite, as well as the abundance of insoluble residues in these carbonates, provide physical support for the weathering hypothesis. The occurrence of this extreme negative biogeochemical event on several cratons suggests that exposure was likely eustatic in origin. If correct, the Rainstorm event could correlate in time to a post-Marinoan (i.e. Gaskiers and equivalents ca. 580 Ma) ice age preserved as glacial diamictites and cap carbonates in Newfoundland (Myrow and Kaufman, 1999; Bowring et al., 2003) and northern Virginia in the USA (Kaufman and Hebert, 2003), or to a younger pre-boundary event for which there is no known glacial record. In either case, it is plausible that rapid oxidation of the oceans and atmosphere and the extreme Rainstorm excursion immediately precede the rapid diversification of Ediacaran

animals, which lie above the biogeochemical anomaly in many of the studied sections (Fig. 4).

5.5. Evolutionary Ramifications

The rise of oxygen in surface environments has long been considered an important environmental stimulus for animal evolution at the end of the Proterozoic Eon (Berkner and Marshall, 1965; Cloud, 1968; Knoll and Carroll, 2000). Model constraints based on coupled isotope systems confirm the view that enhanced burial of organic matter during Pan African orogeny led to the sudden buildup of atmospheric oxygen coincident with the timing of Ediacaran evolution (Derry et al., 1992; Kaufman et al., 1993)(Narbonne et al., 2003). Results of this study of what is arguably the most profound negative carbon isotope anomaly in Neoproterozoic successions are consistent with enhanced levels of oxygen in surface environments and accelerated weathering during sea level regression. Intense weathering of exposed organic-rich marginal marine sediments increased oceanic sulfate and alkalinity, pushing both sulfur and carbon isotope compositions of seawater proxies to negative extremes.

It is noteworthy that the only comparable $\delta^{13}C$ excursion in Precambrian time is recorded in deep-water succession across the Precambrian-Cambrian boundary (Narbonne et al., 1994; Kimura et al., 1997; Bartley et al., 1998; Corsetti and Hagadorn, 2000) separated by only a few million years from the Rainstorm event. We suggest that the biogeochemical anomaly at the boundary (ca. 543 Ma; Bowring et al., 1993; Grotzinger et al., 1995; Amthor et al., 2003) was also driven by oxidative weathering of organic-rich sediments exposed by

sea level regression (Saylor et al., 1998). At this time, however, the oxidative drawdown of atmospheric oxygen resulted in widespread anoxia in the oceans and atmosphere (*cf*. Kimura et al., 1997) and a return of low sulfate concentrations. If correct, the extinction of certain shelly fossils (Amthor et al., 2003) and the disappearance of most Ediacaran forms at this critical boundary may also be coupled to the terminal Proterozoic oscillation of atmospheric oxygen.

6. Conclusions

Open marine carbonates of the Rainstorm Member in the Johnnie Formation of western USA represent an alkalinity anomaly against a background sea of siliciclastic sedimentation. Sudden carbonate deposition at a time of rapid marine transgression implies that seawater alkalinity was so high it drove carbonate deposition in the form of seafloor aragonite cements as well as a background rain of micrite. Given these observations in the siliciclastic-dominated Johnnie Formation and in carbonate-dominated equivalents worldwide, it seems reasonable to assume that atmospheric CO_2 was not so high as to preclude carbonate deposition in both shallow and deep water environments. On the other hand, moderately high pCO_2 (coupled with an enhanced flux of micronutrients, like iron and phosphous, from either the ocean or rivers) may have stimulated primary productivity, resulting in an enhanced rain of carbonate as well as ^{13}C enrichment in organic matter.

Field evidence for significant sea level drawdown and erosion of pre-Rainstorm Johnnie Formation lithologies provides a means for creating the alkalinity required for the carbonate, as well as an explanation for the biogeochemical anomalies. In the proposed

model, exposure of organic matter in marginal marine sediments of the Johnnie Formation to a high O_2 atmosphere enhanced soil CO_2 concentrations. This acidity was neutralized through hydrolysis reactions (e.g. silicate weathering) to form the ^{13}C depleted alkalinity that washed out to sea. A sudden rise in atmospheric O_2 might have also resulted in ventilation of the oceans and oxidation of dissolved organic matter. However, enhanced oceanic CO_2 would likely attenuate carbonate deposition unless alkalinity was formed by microbial processes (for example, sulfide oxidation or methanotrophy) in progressively oxygenated environments.

Geochemical trends in carbon and sulfur isotope abundances, and in sulfate concentrations, in the Rainstorm Member, point to silicate weathering under a high O_2 atmosphere as the source of alkalinity during the profound biogeochemical anomaly. The timing of the O_2 pulse, the isotopically anomalous ^{12}C, ^{32}S, and SO_4^{2-} spikes, and the sudden appearance of Ediacaran fossils demonstrates how external geosystem factors (tectonics, climate, sedimentation and productivity) may have driven early animal evolution and extinction.

Acknowledgements

We wish to acknowledge John Cooper and Chris Fedo for their observations of the Johnnie Oolite in the Old Dad Mountains, as well as Pedro Marenco, Alison Olcott, and Nate Lorentz who provided new insights to the CAS extraction procedures. This research was supported by grants from the National Science Foundation and NASA-Exobiology as well as

internal grants to AJK and FAC from the University of Maryland and University of Southern California, respectively.

References

Abolins, M., Oskin, R., Prave, T., Summa, C. and Corsetti, F.A., 2000. Neoproterozoic glacial record in the Death Valley region, California and Nevada. In: Lagerson, D.R., Peters, S.G., Lahren, M.M. (Eds.), Great Basin and Sierra Nevada. Geol. Soc. Am. Field Guide, 2000, vol. 2, pp. 319-335.

Aharon, P., Fu, Baoshun, 2003. Sulfur and oxygen isotopes of coeval sulfate-sulfide in pore fluids of cold seep sediments with sharp redox gradients. Chem. Geol. 195, 201-218.

Amthor, J.E., Grotzinger, J.P., Schroeder, S., Bowring, S.A., Ramezani, J., Martin, M.W., Matter, A., 2003. Extinction of Cloudina and Namacalathus at the Precambrian-Cambrian boundary in Oman. Geology 31, 431-434.

Andrews, J.A., Schlesinger, W.H., 2001. Soil CO_2 dynamics, acidification, and chemical weathering in a temperate forest with experimental CO_2 enrichment. Global Biogeochem. Cycles 15**,** 149-162.

Arthur M.A., 2000. Volcanic contributions of the carbon and sulfur geochemical cycles and global change. In: Sigurdsson, H., Houghton, B.F., McNutt, S.R., Rymer, H., Stix, J. (Eds.) Encyclopedia of Volcanoes, pp. 1045-1056.

Banner, J.L., Hanson, G.N., 1990. Calculation of simultaneous isotopic and trace element variations during water-rock interaction with applications to carbonate diagenesis. Geochim. Cosmochim. Acta 54, 3123-3137.

Bartley, J.K. and Kah, L.C., 2004. Marine carbon reservoir, C_{org} -C_{carb} coupling, and the evolution of the Proterozoic carbon cycle. Geology 32, 129-132.

Bartley, J.K., Pope, M., Knoll, A.H., Semikhatov, M.A., Petrov, P. Yu, , 2001. A Vendian-Cambrian boundary succession from the northwestern margin of the Siberian Platform; stratigraphy, palaeontology, chemostratigraphy and correlation. Geol. Mag. 135, 473-494.

Benmore, W.C., 1974. Stratigraphy and paleoecology of the lower Johnnie Formation, southern Nopah Range, eastern California. M.S. thesis, University of California, Santa Barbara. p.

Benmore, W.C., 1978. Stratigraphy, sedimentology, and paleoecology of the late Paleophytic or earliest Phanerozoic Johnnie Formation, eastern California and southwestern Nevada. Ph.D. thesis, University of California, Santa Barbara, 263 p.

Berkner , L.V., Marshall, L.C., 1965. History of major atmospheric components. Proc. Natl. Acad. Sci. USA 53, 1215-1226

Berner, R.A., 2001. Modeling atmospheric O_2 over Phanerozoic time. Geochim. Cosmochim. Acta 65, 685-694.

Boetius, A., Ravenschlag, K., Schubert, C. J., Rickert, D., Widdel, F., Gieseke, A., Amann, R., Jorgensen, B.B., Witte, U., Pfannkuche, O., 2000. A marine microbial consortium apparently mediating anaerobic oxidation of methane. Nature 407, 623-626.

Bowring, S.A., Grotzinger, J.P., Isachsen, C.E., Knoll, A.H., Pelechaty, S.M., Kolosov, P., 1993. Calibrating rates of Early Cambrian evolution. Science 261, 1293-1298.

Bowring, S.A., Myrow, P.M., Landing, E., Ramezani, J., Condon, D., Hoffmann, K.H., 2003. Geochronological constraints on Neoproterozoic glaciations and the rise of metazoans. Geol. Soc. Am. 35, 516, Program with Abstracts.

Burdett J.W., Arthur M.A., Richardson M., 1989. A Neogene seawater sulfur isotope age curve from calcareous pelagic microfossils. Earth Planet. Sci. Lett. 94**,** 189-198.

Burns, S.J., Matter, A., 1993. Carbon isotopic record of the latest Proterozoic from Oman. Eclogae Geol. Helv. 86, 595–607.

Calver, C.R., 2000, Isotope stratigraphy of the Ediacarian (Neoproterozoic III) of the Adelaide rift complex, Australia, and the overprint of water column stratification: Precambrian Res. 100, 121–150.

Canfield, D.E., 1998. A new model for Proterozoic ocean chemistry. Nature **396,** 450-452.

Canfield, D.E., Teske, A., 1996. Late Proterozoic rise in atmospheric oxygen concentration inferred from phylogenetic and sulphur-isotope studies. Nature 382, 127-132.

Charlton, R.L., Wernicke, B.P., Abolins, M.J., 1997. A major Neoproterozoic incision event near the base of the Cordilleran miogeocline, southwestern Great Basin. Geol. Soc. Am. 29, 197, Program with Abstracts.

Christie-Blick, N., Levy, M., 1989. Stratigraphic and tectonic framework of upper Proterozoic and Cambrian rocks in the Western United States. In: Christie-Blick, N., Levy, M., Mount, J.F., Signor, P.W., Link, P.K. (Eds.), Late Proterozoic and

Cambrian tectonics, sedimentation, and record of metazoan radiation in the Western United States. 28th Int. Geol. Cong. field trip guide series 7-21, 113 p.

Christie-Blick, N.C., von der Borch, C.C., Dibona, P.A., 1990. Working hypotheses for the origin of the Wonoka canyons (Neoproterozoic), South Australia. Am. J. Sci. 290-A, 295-332.

Christie-Blick, N.C., Dibona, P.A., von der Borch, C.C., 1995. Sequence stratigraphy and the interpretation of Neoproterozoic Earth history. Precambrian Res. 73, 3-26.

Clapham, M.E., Corsetti, F.A., 2004. Tectonically-driven deep valley incision in the terminal Neoproterozoic Johnnie Formation, eastern California. Geol. Soc. Am., in press, Program with Abstracts.

Claypool, G.E., Holser, W.T., Kaplan, I.R., Sakai, H., Zak, I., 1980. The age curves of sulfur and oxygen isotopes in marine sulfate and their mutual interpretation. Chem. Geol. 28, 199-260.

Cloud, P.E., 1968. Atmospheric and hydrospheric evolution on the primitive Earth. Science 160, 729-736.

Corsetti, F.A., Hagadorn, J.W., 2000. Precambrian–Cambrian transition: Death Valley, United States. Geology 28, 299–302.

Corsetti, F.A., Kaufman, A.J., 2003. Stratigraphic investigations of carbon isotope anomalies and Neoproterozoic ice ages in Death Valley, California. Geol. Soc. Am. Bull. 115, 916-932.

Corsetti, F.A., Lorentz, N.J., Pruss, S.B., in press. Formerly-Aragonite Seafloor Fans from Neoproterozoic Strata, Death Valley and Southeastern Idaho, United States: Implications for "Cap Carbonate" Formation and Snowball Earth. In: Jenkyns, G., Sohl, L. (Eds.) AGU Monograph.

Derry L.A., Kaufman A.J., Jacobsen S.B., 1992. Sedimentary cycling and environmental change in the Late Proterozoic: evidence from stable and radiogenic isotopes. Geochim. Cosmochim. Acta 59, 1317-1329.

Des Marais, D.J., Strauss, H., Summons, R.E., Hayes, J.M., 1992. Carbon isotope evidence for the stepwise oxidation of the Proterozoic environment. Nature 359, 605-609.

Dickens G.R., Castillo M.M., Walker J.C.G., 1995. Discussion of oceanic methane hydrate as a cause of the carbon isotope excursion at the end of the Paleocene. Paleoceanography 10**,** 965-971.

Fedo, C.M., Cooper, J.D., 2001. Sedimentology and sequence stratigraphy of Neoproterozoic and Cambrian units across a craton-margin hinge zone, southeastern California, and implications for the early evolution of the Cordilleran margin. Sediment. Geol. 141-142, 501-522.

Fung, I.Y., John. J., Lerner, J., Matthews, E., Prather, M., Steele, L.P., Fraser. P.J., 1991. Three-dimensional model synthesis of the global methane cycle. J. Geophys. Res., D, Atmospheres 96, 13,033-13,065.

Gellatly, A.M., Lyons, T.W., Kah, L.C., 2001. Carbonate-associated sulfate in Mesoproterozoic successions and modern carbonate systems; examining rapid shifts in paleoenvironmental conditions. Geol. Soc. Am. 33, 95, Program with Abstracts.

Grassineau, N.V., Mattey, D.P., Lowry, D., 2001. Sulfur isotope analysis of sulfide and sulfate minerals by continuous flow-isotope ratio mass spectrometry. Anal. Chem. 73, 220-225.

Grey, K., Walter, M.R., Calver, C., 2003. Neoproterozoic biotic diversification; snowball Earth or aftermath of the Acraman impact? Geology 31, 459-462.

Grotzinger, J.P., Bowring, S.A., Saylor, B.Z., Kaufman, A.J., 1995. Biostratigraphic and geochronologic constraints on early animal evolution. Science 270, 598-604.

Hagadorn, J.W., Fedo, C.M., Waggoner, B.M., 2000. Early Cambrian Ediacaran-type fossils from California. J. Paleontol. 74, 731-740.

Hayes, J.M., Kaplan, I.R., Wedeking, K.W., 1983. Precambrian organic geochemistry, preservation of the record. In: Schopf, J.W. (Ed.) The Earth's Earliest Biosphere: Its Origin and Evolution. Princeton University Press, Princeton, NJ, pp. 93-134.

Hayes, J.M., Strauss, H., Kaufman, A.J., 1999. The abundance of ^{13}C in marine organic matter and isotopic fractionation in the global biogeochemical cycle of carbon during the past 800 Ma. Chem. Geol. 161, 103–125.

Heaman, L.M., Grotzinger, J.P., 1992. 1.08 Ga diabase sills in the Pahrump Group, California: Implications for development of the Cordilleran miogeocline. Geology 20, 637–640.

Hoffman, P.F., Kaufman, A.J., Halverson, G.P., Schrag, D.P., 1998. A Neoproterozoic snowball Earth. Science 281, 1342–1346.

Holser, W.T., 1984. Gradual and abrupt shifts in ocean chemistry during Phanerozoic time. In: Holland, H.D., Trendall, A.F. (Eds.) Patterns of Change in Earth Evolution. Dahlem Workshop, Berlin, Germany, pp. 123-143.

Hurtgen, M.T., Arthur, M.A., Suits, N.S., Kaufman, A.J., 2002. The sulfur isotopic composition of Neoproterozoic seawater sulfate; implications for a snowball Earth? Earth Planet. Sci. Lett. 203, 413-429.

Irwin, H., Curtis, C., Coleman, M., 1977. Isotopic evidence for source of diagenetic carbonates formed during burial of organic-rich sediments. Nature 269, 209-213.

Iverson, N., 1996. Methane oxidation in coastal marine environments. In: Murrell, J.C., Kelly, D.P. (Eds.) Microbiology of Atmospheric Trace Gases. Springer-Verlag, Berlin, pp. 51-68.

Iyer, S.S., Babinski, M., Krouse, H.R., Chamale, F., Jr., 1995. Highly ^{13}C enriched carbonate and organic matter in the Neoproterozoic sediments of the Bambuí Group, Brazil. Precambrian Res. 73**,** 271-282.

Jacobsen, S.B., 2001. Gas hydrates and deglaciations. Nature 412, 691-693.

Jacobsen, S.B. Kaufman, A.J., 1999. The Sr, C, and O isotopic evolution of Neoproterozoic seawater. Chem. Geol. 161**,** 37-57.

Jiang, Ganqing, Christie-Blick, N., Kaufman, A.J., Banerjee, D.M., Rai, V., 2002. Sequence stratigraphy of the Neoproterozoic Infra Krol Formation and Krol Group, Lesser Himalaya, India. J. Sediment. Res. 72, 524-542.

Jiang, Ganqing, Kennedy, M.J., Christie-Blick, N., 2004, Stable isotopic evidence for methane seeps in Neoproterozoic postglacial cap carbonates. Nature 426, 822-826.

Karlstrom, K.E., Bowring, S.A., Dehler, C.M., Knoll, A.H., Porter, S.M., Des Marais, D.J., Weil, A.B., Sharp, Z.D., Geissman, J.W., Elrick, M.B., Timmons, J.M., Crossey, L.J., Davidek, K.L., 2000. Chuar Group of the Grand Canyon: Record of breakup of Rodinia, associated change in the global carbon cycle, and ecosystem expansion by 740 Ma. Geology 28, 619–622.

Kampschulte, A., Bruckschen, P., Strauss, H., 2001. The sulphur isotopic composition of trace sulphates in Carboniferous brachiopods: implications for coeval seawater, correlation with other geochemical cycles and isotope stratigraphy. Chem. Geol. 175, 165-198.

Kampschulte, A., Strauss, H., 2004. The sulfur isotopic evolution of Phanerozoic seawater based on the analysis of structurally substituted sulfate in carbonates. Chem. Geol.

Kaufman, A.J., Hayes, J.M., Knoll, A.H., Germs, G.J.B., 1991. Isotopic compositions of carbonates and organic carbon from upper Proterozoic successions in Namibia:

Stratigraphic variation and the effects of diagenesis and metamorphism. Precambrian Res. 49, 301–327.

Kaufman, A.J., Jacobsen, S.B., Knoll, A.H., 1993. The Vendian record of C- and Sr-isotopic variations: Implications for tectonics and paleoclimate. Earth Planet. Sci. Lett. 120, 409-430.

Kaufman, A.J., Knoll, A.H., Narbonne, G.M., 1997. Isotopes, ice ages, and terminal Proterozoic Earth history. Proc. Natl. Acad. Sci.. 94, 6600–6605.

Kaufman, A.J., Jiang, G., Christie-Blick, N., Banergee, D.M., Rai, V., 2000. A terminal Proterozoic history of sea level change and biogeochemical anomalies, Lesser Himalaya, India. Geol. Soc. Am. 32, 94, Abstracts with Programs.

Kaufman, A.J., Varni, M., Wing, B., 2002. Sulfur isotope constraints on the Snowball Earth. Geol. Soc. Am., Program with Abstracts.

Kaufman, A.J., Hebert, C.L., 2003. Stratigraphic and radiometric constraints on rift-related volcanism, terminal Neoproterozoic glaciation, and animal evolution. Geol. Soc. Am. 35, 516, Program with Abstracts.

Kaufman, A.J., Knoll, A.H., 1995. Neoproterozoic variations in the C-isotopic composition of seawater; stratigraphic and biogeochemical implications. Precambrian Res. 73, 27–49.

Kennedy, M.J., Christie-Blick, N., and Sohl, L.E., 2001, Are Proterozoic cap carbonates and isotopic excursions a record of gas hydrate destabilization following Earth's coldest intervals? Geology 29, 443–446.

Kimura, H., Matsumoto, R., Kakuwa, Y., Hamdi, B., Zibaseresht, H., 1997. The Vendian-Cambrian $\delta^{13}C$ record, North Iran; evidence for overturning of the ocean before the Cambrian explosion. Earth Planet. Sci. Lett. 147, E1-E7.

Knoll, A.H., Carroll, S.B., 1999. Early animal evolution: emerging views from comparative biology and geology. Science 284, 2129–2137.

Knoll, A.H., Hayes, J.M., Kaufman, A.J., Swett, K., Lambert, I.B., 1986. Secular variation in carbon isotope ratios from upper Proterozoic successions of Svalbard and East Greenland. Nature 321, 832–838.

Kvenvolden, K.A., 1995. A review of the geochemistry of methane in natural gas hydrate. Organic Geochem. 23, 997-1008.

Moore, J.N., 1974, Stratigraphic comparison of the Precambrian Wyman and Johnnie Formations in the western Great Basin, California: Geological Society of America Abstracts with Programs, v. 6, no. 3, p. 222–223.

McKirdy, D.M., Burgess, J.M., Lemon, N.M., Yu, X., Cooper, A.M., Gostin, V.A., Jenkins, R.J.F., and Both, R.A., 2001, A chemostratigraphic overview of the late Cryogenian interglacial sequence in the Adelaide fold-thrust belt, South Australia: Precambrian Research, v. 106, p. 149–186.

Myrow, P., Kaufman, A.J., 1999. A newly-discovered cap carbonate above Varanger-aged glacial deposits in Newfoundland. J. Sed. Res. 69, 784-793.

Narbonne, G., Kaufman, A.J., Knoll, A.H., 1994. Integrated Carbon Isotope and Biostratigraphy of the Upper Windermere Group, MacKenzie Mountains, N.W. Territories, Canada. Geol. Soc. Am. Bull. 106, 1281-1292.

Narbonne, G.M., Gehling, J.G., 2003. Life after snowball; the oldest complex Ediacaran fossils. Geology 31, 27-30.

Newton, R.J., Pevitt, E.L., Wignall, P.B., Bottrell, S.H., 2004. Large shifts in the isotopic composition of seawater sulphate across the Permo-Triassic boundary in northern Italy. Earth Planet. Sci. Lett. 218, 331-345.

Olcott, A., Lorentz, N.J., Corsetti, F.A., Berelson, W., 2004. Reevaluating gravimetric determination of carbonate associated sulfate concentrations. Geol. Soc. Am., in press, Program with Abstracts.

Olson, J.S., Garrels, R.M., Berner, R.A., Armentano, T.V., Dyer, M.I., Yaalon, D.H., 1985. The natural carbon cycle. In: Trabalka, J.R. (Ed.) Atmospheric Carbon Dioxide and the Global Carbon Cycle. Oak Ridge Natl. Lab., Oak Ridge, TN, United States, pp.175-213.

Pavlov, A.A., Hurtgen, M.A., Kasting, J.F., Arthur, M.A., 2003. Methane-rich Proterozoic atmosphere? Geology 31, 87-90.

Pell, S.D., McKirdy, D.M., Jansyn, J., Jenkins, R.J.F., 1993. Ediacaran carbon isotope stratigraphy of South Australia – an initial study. Trans. R. Soc. S. Aust. 117, 153-161.

Petsch, S.T., Berner, R.A., Eglinton, T.I., 2000. A field study of the chemical weathering of ancient sedimentary organic matter. Organic Geochemistry 31**,** 475-487.

Pruss, S.B., Corsetti, F.A., 2002. Unusual aragonite precipitates in the Neoproterozoic Rainstorm Member of the Johnnie Formation. In: Corsetti, F.A. (Ed.) Proterozoic-

Cambrian of the Great Basin and Beyond 93, Fullerton, California, Pacific Section SEPM, p. 51-60.

Reeburgh, W.S., Ward, B.B., Whalen, S.C., Sandbeck, K.A., Kilpatrick, K.A., Kerkhof, L.J., 1991. Black Sea methane geochemistry. In: Murray, J.W. (Ed.) Black Sea oceanography; results from the 1988 Black Sea Expedition. Deep-Sea Research. Part A: Oceanographic Research Papers, 1991, Vol. 38, Issue Suppl. 2A, pp. 1189-1210.

Rothman, D.H., Hayes, J.M., Summons, R.E., 2003. Dynamics of the Neoproterozoic carbon cycle. Proc. Natl. Acad. Sci. USA 100, 8124-8129.

Saylor, B.Z., Kaufman, A.J., Grotzinger, J.P., Urban, F., 1998. A composite reference section for terminal Neoproterozoic strata of southern Namibia. J. Sediment. Res. 68, 1223-1235.

Schmidt, P.W., Williams, G.E., 1996. Palaeomagnetism of the ejecta-bearing Bunyeroo Formation, late Neoproterozoic, Adelaide fold belt, and the age of the Acraman impact. Earth Planet. Sci. Lett. 144, 347-357.

Shapiro, R.S., 2002. Are Proterozoic cap carbonates and isotopic excursions a record of gas hydrate destabilization following Earth's coldest intervals? Geology 30, 761-762.

Strauss, H., 1993. The sulfur isotope record of Precambrian sulfate: new data and a critical evaluation of the existing record. Precambrian Res. 63**,** 225-246.

Strauss, H., 1997. The isotopic composition of sedimentary sulfur through time. Palaeogeo., Palaeoclimat., Palaeoecol. 132**,** 97-118.

Stewart, J.H., 1970, Upper Precambrian and Lower Cambrian strata in the southern Great Basin, California and Nevada: U.S. Geol. Surv. Prof. Pap. 620, 206 p.

Stewart, J.H., 1982. Regional relations of Proterozoic Z and Lower Cambrian rocks in the Western United States and northern Mexico. In: Cooper, J.D., Troxel, B.W., and Wright, L.A. (Eds.), Geology of Selected Areas in the San Bernardino Mountains, western Mojave Desert, and southern Great Basin, California. Geol. Soc. Am. Codilleran Section Volume and Guidebook: Shoshone, CA, Death Valley Publ, Co, p. 171-180.

Summa, C.L., Southard, J.B., Grotzinger, J.P., 1991. Stratigraphy and sedimentology of the late Proterozoic Johnnie Formation, eastern California and western Nevada. In: Anonymous (Ed.) Geological Society of America, 1991 annual meeting, Volume 23, Geological Society of America (GSA), p. 347.

Summa, C.L., 1993a. Sedimentologic, stratigraphic, and tectonic controls of a mixed carbonate-siliciclastic succession: Neoproterozoic Johnnie Formation, southeast California. Ph.D. thesis, Massachusetts Institute of Technology, 616 p.

Summa, C.L., Southard, J.B., Grotzinger, J.P., 1993b, Distinctive cross-stratification in amalgamated storm event beds: Neoproterozoic upper Johnnie Formation, eastern California: Geol. Soc. Am. 25, 67, Abstracts with Programs.

Valentine, J.W., 2002. Prelude to the Cambrian explosion. Ann. Rev. Earth Planet. Sci. 30, 285-306.

Von der Borch, C.C., Grady, A.E., Eickhoff, K.H., Dibona, P.A., Christie-Blick, N., 1989. Late Proterozoic Patsy Springs Canyon, Adelaide Geosyncline; submarine origin? Sedimentol. 36, 777-792.

Varni, M. A., Kaufman, A.J., Misi, A., Brito Neves, B.B., 2001. Anomalous $\delta^{34}S$ signatures in trace sulfate from a potential cap carbonate in the Neoproterozoic Bambuí Group, Brazil. Geol. Soc. Am. 33, A-96, Program with Abstracts.

Veizer, J., Ala, D., Azmy, K., Bruckschen, P., Buhl, Dieter; Bruhn, F., Carden, G.A.F., Diener, A., Ebneth, S., Godderis, Y., Jasper, T., Korte, C., Pawellek, F., Podlaha, O.G., Strauss, H., 1999. $^{87}Sr/^{86}Sr$, $\delta^{13}C$ and $\delta^{18}O$ evolution of Phanerozoic seawater. Chem. Geol. 161, 59-88.

Wakeham, S.G., Hopmans, E.C., Schouten, S., Sinninghe Damsté, J.S., in press. Archaeal lipids and anaerobic oxidation of methane in euxinic water columns: a comparative study of the Black Sea and Cariaco Basin. Chem. Geol.

Zhou, Chuanming, Tucker, R., Xiao, Shuhai, Peng, Zhanxiong, Yuan, Xunlai, Chen, Zhe, 2004. New constraints on the ages of Neoproterozoic glaciations in south China. Geology 32, 437-440.

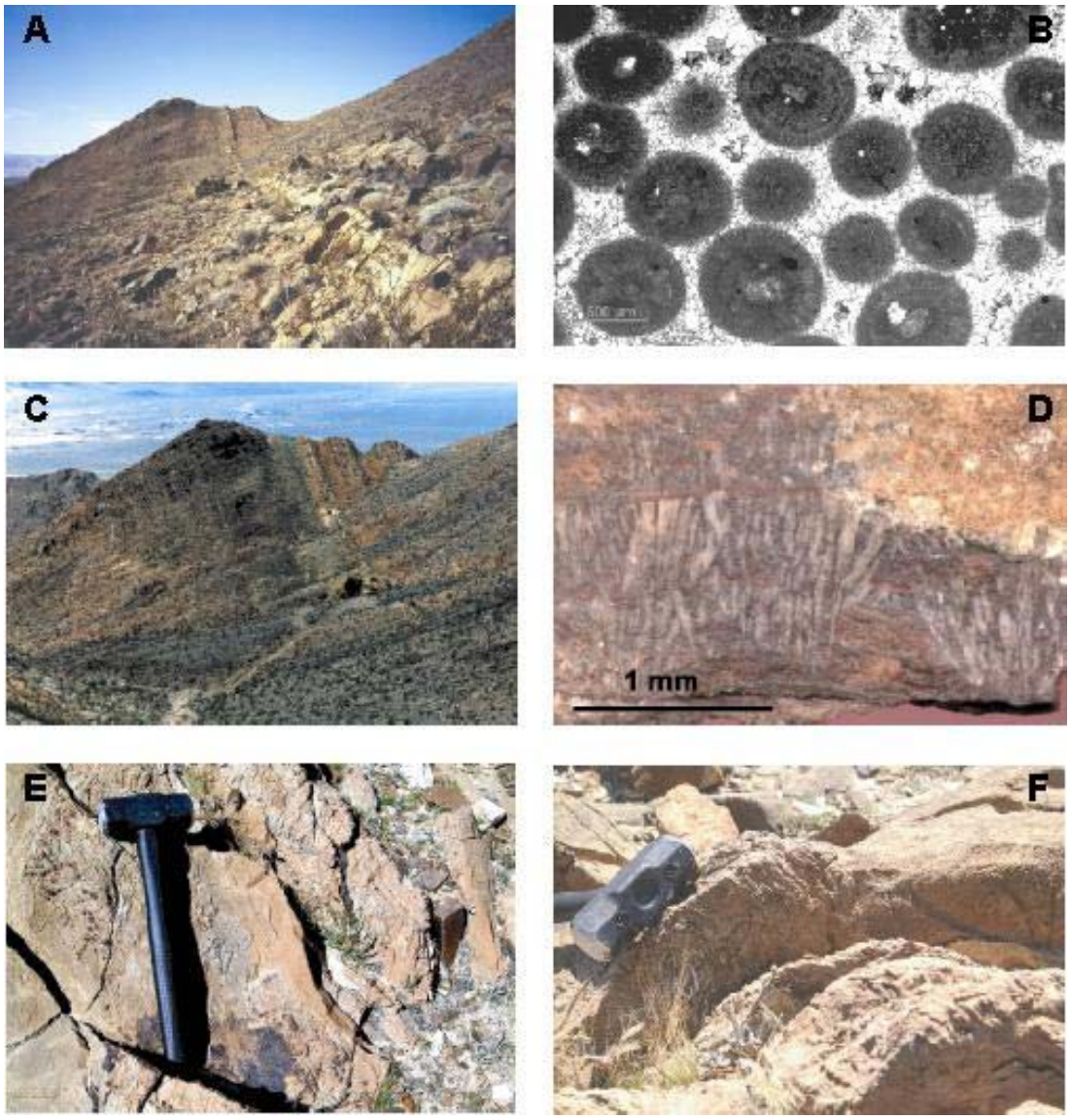

Fig 1: Field and thin section photographs of the Johnnie Oolite and Rainstorm carbonates: (A) the lonesome Johnnie Oolite; (B) concentric dolomite ooids of the Johnnie Formation with ~ 30% isopachous and sparry calcite cement; (C) Pink to orange carbonate of the Rainstorm above the oolite and dark grey to green silts and shales of the Johnnie Formation; (D) Neomorphosed (previously aragonite) seafloor cements from the Rainstorm Member carbonates; (E and F) karst of grey stromatolitic dolomite infilled by the Johnnie Oolite.

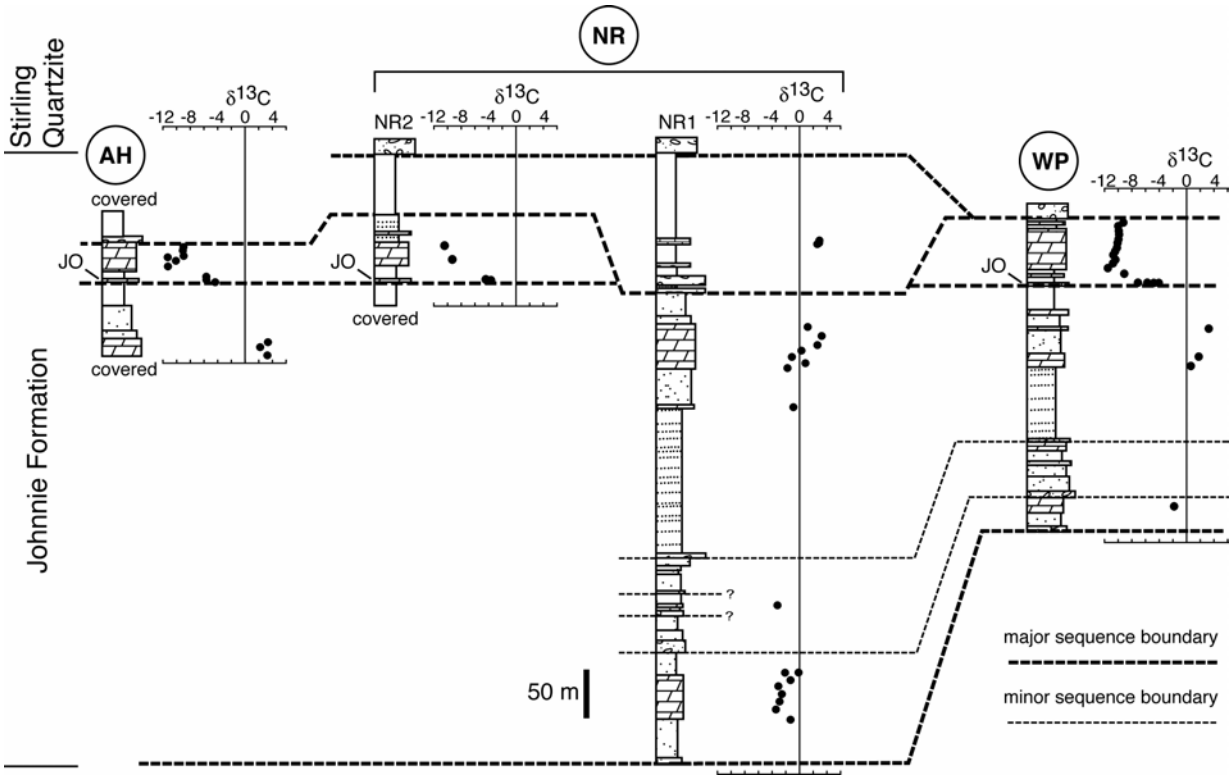

Fig. 2. Chemostratigraphy of the Johnnie Formation (localities shown in Corsetti and Kaufman, 2003) with section from the Alexander Hills (AH), Nopah Range (NR1 and NR2), and Winters Pass Hills (WP). Note that the incised valley has removed the Rainstorm Member carbonates along strike. JO – Johnnie Oolite.

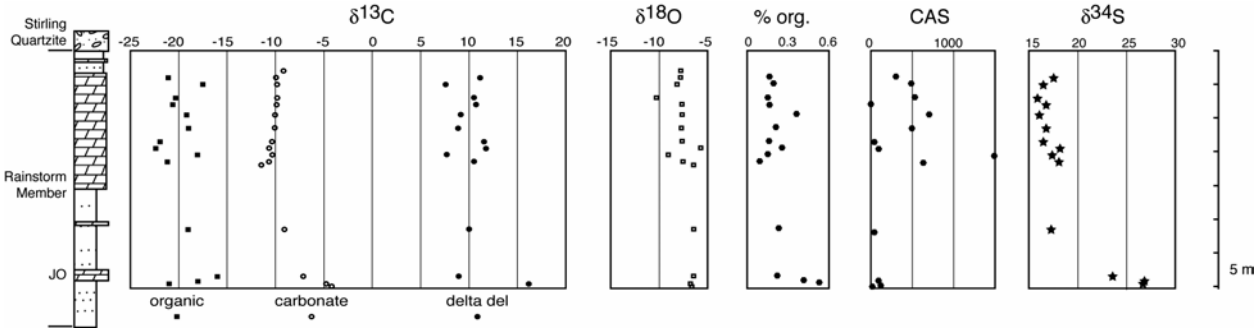

Fig. 3. High resolution chemostratigraphy of the Rainstorm Member at Winters Pass Hills.

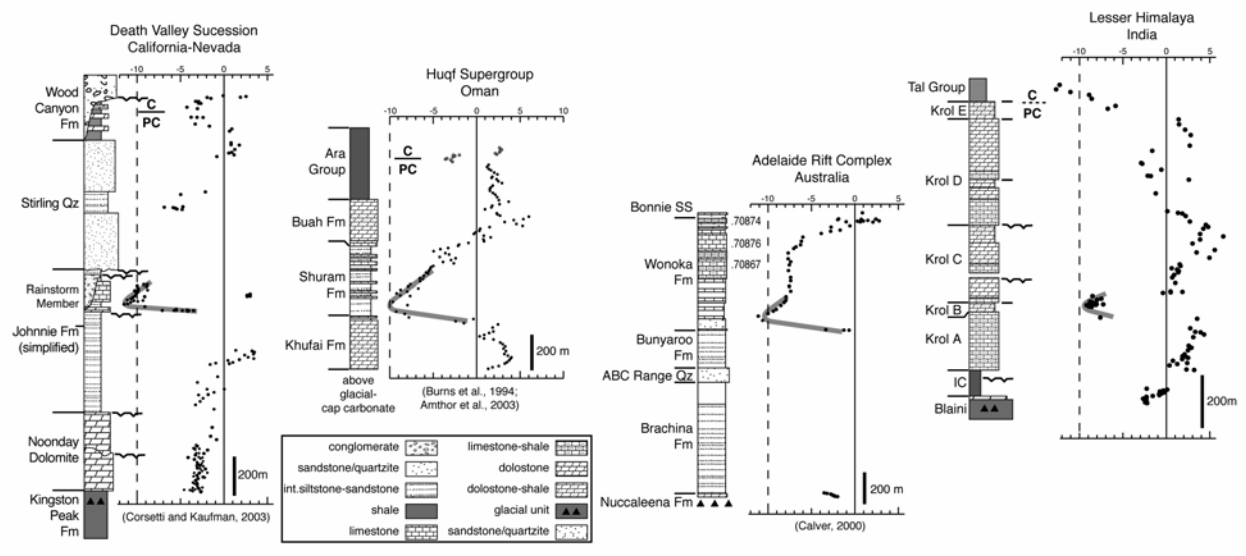

Fig. 4. Proposed global correlation of the extreme negative carbon isotope anomaly recorded in the terminal Neoproterozoic Rainstorm Member carbonates. The event lies stratigraphically above diamictites of assumed Marinoan age and below the first occurrence of Ediacaran animals and the Precambrian-Cambrian boundary in all successions.

Table 1: Elemental and isotopic compositions of Johnnie Formation carbonates, Death Valley, USA

sample	description	$\delta^{13}C$ (‰ VPDB)	$\delta^{18}O$ (‰ VPDB)	$\delta^{13}Corg$ (‰ VPDB)	$\Delta\delta^{13}C$ (‰ VPDB)	TOC (mg/g)	residue (%)	CAS* (ppm)	$\delta^{34}S$ (‰ CDT)
Winters Pass Hills									
C99-136	dol. oolite	-4.80	-7.39	-20.93	16.13	0.53	3.7	17.0	26.6
C99-137	dol. oolite	n.d.	n.d.	-18.02	n.d.	0.41	6.2	122.5	26.7
C99-138	dol. oolite	-7.13	-7.05	-16.01	8.88	0.22	8.4	94.1	23.5
C99-139	micrite	-9.12	-7.04	-19.04	9.92	0.23	19.9	41.9	17.2
C99-144	micrite	-10.75	-8.17	-21.14	10.39	0.09	18.1	636.3	18.0
C99-145	micrite	-10.38	-9.68	-18.06	7.68	0.15	40.1	1490.7	17.3
C99.146	micrite	-10.69	-6.33	-22.36	11.67	0.25	24.7	101.3	18.1
C99-147	micrite	-10.43	-8.22	-21.92	11.49	0.16	10.0	43.6	16.4
C99-148	micrite	-10.16	-8.32	-19.00	8.84	0.21	11.4	495.1	16.7
C99-149	micrite	-10.09	-8.23	-19.20	9.11	0.36	10.7	708.0	16.0
C99-150	micrite	-9.95	-8.27	-20.64	10.69	0.16	22.4	5.5	16.7
C99-151	micrite	-9.87	-10.89	-20.31	10.44	0.15	19.9	535.5	15.8
C99.152	micrite	-9.92	-8.78	-17.49	7.57	0.19	11.8	488.7	16.4
C99-153	micrite	-9.99	-8.42	-21.08	11.09	0.16	15.1	304.5	17.5
Alexander Hills									
AR 1	grey dol.	3.0	-3.7						
AR 4	grey dol.	2.7	-5.0						
AR 5	black dol.	3.1	-8.5						
AR 10	dol. oolite	-4.1	-7.6						
AR 11	dol. oolite	-5.3	-7.7						
AR 12	dol. oolite	-5.6	-6.8						
AR 13	micrite	-10.2	-15.5						
AR 15	crystal fan lms.	-9.5	-15.5						
AR 16	micrite	-9.0	-13.0						
AR 17	micrite	-10.2	-15.9						
AR 18	micrite	-8.6	-14.2						
AR 19	micrite	-8.8	-14.6						
AR 21	breccia clast	-8.8	-14.9						
AR 21	micrite	-9.2	-15.3						

Southern Nopah Range, section 1 of Corsetti and Kaufman (2003)

RS 142	micrite	2.6	-15.5	-24.16	26.8
RS 143	micrite	2.9	-16.8	-21.01	23.9
RS 145	micrite	2.6	-13.5	-20.01	22.6
RS 146	micrite	2.9	-15.0		

Southern Nopah Range, section 2 of Corsetti and Kaufman (2003)

JF 15	dolarenite	-1.3	-4.5		
JF 16	dolarenite	-3.5	-6.7		
JF 17	dolomicrite	-2.9	-5.8		
JF 19	dolomicrite	-2.6	-6.9		
JF 21	dolomicrite	-3.1	-7.3		
JF 22	dolomicrite	-1.3	-5.6		
JF 23	strom. dol.	-2.1	-5.7		
JF 25	strom. dol.	-0.1	-7.1		
JF 26	dol. grainstone	-3.2	-11.1		
JF 27	dolomicrite	-0.9	-5.3		
JF 28	dolomicrite	-1.8	-7.5	-21.01	19.3
JF 29	caliche	0.9	-6.9	-21.34	22.2
JF 30	dolomicrite	-1.1	-5.5		
JF 31	dolomicrite	0.3	-1.9	-22.18	22.4
JF 32	dolomicrite	2.6	-7.5		
JF 33	microbial dol.	3.3	-5.4		
JF 34	dolomicrite			-19.96	
JF 36	microbial dol.	1.2	-5.1		
JF 37	dol. oolite	-3.7	-7.0	-17.90	14.2
RS 39	micrite	-9.3	-12.6	-19.34	10.0
RS 40	crystal fan lms.	-10.4	-14.2		

Old Dad Mountains

ODM-1	lam. dol.	-2.33	-8.33
ODM-2-1	strom. dol	-2.33	-7.21
ODM-2-2	dol. oolite	-3.65	-9.59
ODM-2-3	strom. dol	-2.70	-7.62
ODM-4-1	dol. oolite	-5.60	-13.64
ODM-4-2	dol. oolite	-3.19	-8.58

*CAS abundance calculated on a siliciclastic free basis
n.d. = not determined

Table 2: XRD mineralogic compositions* of insoluble residues from Johnnie Formation carbonates at Winters Pass Hills, Death Valley, USA

C99-139	**quartz** > muscovite > chlorite . montmorillonite
C99-145	**quartz** > sanidine > microcline > albite > orthoclase
C99-136	**quartz** > muscovite > phlogopite > biotite > illite
C99-150	**quartz** > albite > anothoclase > sanidine > chlorite
C99-148	**quartz** > microcline > orthoclase > albite > chlorite

* XRD analysis reveals that almost all ($95\%^{+}$) of the insoluble residue collected after dissolving carbonate in 3M HCl is quartz with only trace amounts of other minerals.